

# We are IntechOpen, the world's leading publisher of Open Access books Built by scientists, for scientists

6,900

Open access books available

185,000

International authors and editors

200M

Downloads

Our authors are among the

154

Countries delivered to

TOP 1%

most cited scientists

12.2%

Contributors from top 500 universities



WEB OF SCIENCE™

Selection of our books indexed in the Book Citation Index  
in Web of Science™ Core Collection (BKCI)

Interested in publishing with us?  
Contact [book.department@intechopen.com](mailto:book.department@intechopen.com)

Numbers displayed above are based on latest data collected.  
For more information visit [www.intechopen.com](http://www.intechopen.com)



# Higher Order Haar Wavelet Method for Solving Differential Equations

*Jüri Majak, Mart Ratas, Kristo Karjust and Boris Shvartsman*

## Abstract

The study is focused on the development, adaption and evaluation of the higher order Haar wavelet method (HOHWM) for solving differential equations. Accuracy and computational complexity are two measurable key characteristics of any numerical method. The HOHWM introduced recently by authors as an improvement of the widely used Haar wavelet method (HWM) has shown excellent accuracy and convergence results in the case of all model problems studied. The practical value of the proposed HOHWM approach is that it allows reduction of the computational cost by several magnitudes as compared to HWM, depending on the mesh and the method parameter values used.

**Keywords:** higher order Haar wavelet method, convergence analysis, accuracy estimates, improvement of widely used Haar wavelet method

## 1. Introduction

Wavelets are most commonly used in signal processing applications to denoise the real signal, to cut a signal into different frequency components, to analyze the components with a resolution matched to its scale, also in image compression, earthquake prediction and other algorithms.

However, the current study is focused on the area where the use of wavelet methods shows a growth trend, i.e., in the solution of differential equations. Many different wavelets based methods have been introduced for solving differential and integro-differential equations. The Legendre wavelets are utilized to solve fractional differential equations in [1–4] and integro-differential equations in [5, 6]. In [7, 8], the Daubechies wavelet based approximation algorithms are derived to solve ordinary and partial differential equations. In [9], the Lucas wavelets are combined with Legendre–Gauss quadrature for solving fractional Fredholm–Volterra integro-differential equations. The series solution of partial differential equations through separation of variables is developed by using the Fourier wavelets in [10]. The Riesz wavelets- based method for solving singular fractional integro-differential equations was developed in [11]. In the studies in [12], the Galerkin method was combined with the quadratic spline wavelets for solving Fredholm linear integral equations and second-order integro-differential equations. The Chebyshev wavelets method for partial differential equations with boundary conditions of the telegraph type is examined in [13].

The simplest of all wavelet-based approaches was introduced by Alfred Haar already in 1910 [14]. The Haar wavelet-based approach for solving differential and integro-differential equations was introduced in 1997 [15, 16]. Based on the Haar wavelet method (HWM), Chen and Hsiao in [15, 16] proposed an approach where the higher order derivative involved in the differential or integro-differential equations is expanded into the series of Haar wavelets. This approach is based on the nature of Haar functions. Due to the piece-wise constant nature of the Haar functions they are not differentiable but are integrable. In [15, 16], the problems of the lumped and distributed parameter system and those of linear time delayed systems were solved. The Chen and Hsiao approach-based HWM was adapted successfully for solving a wide class of differential, integro-differential and integral equations [17–45]. Pioneering work in the development of Haar wavelet-based techniques was conducted by Lepik [17–23], covering ordinary and partial differential equations [17, 19, 21], integro-differential equations [18], integral equations [20], and fractional integral equations [22]. The HWM approaches and their applications are summarized in a monograph [23]. The HWM is adapted for the analysis of nonlinear integral and integro-differential equations in [24–27], covering one- and multi-dimensional problems. Solid mechanics, particularly composite structures, are examined using the HWM in [28–33]. These studies cover free vibration analysis of orthotropic plates [28], functionally graded composite structures [30–32], delamination detection in composite beams [29], and other structures.

Some recent trends in the development and application of the HWM can be outlined as solutions of fractional differential and integro-differential equations [34–38] as well as the development of a non-uniform and adaptive grid. In the case of fractional differential or integro-differential equations, two principally different HWM approaches regarding to wavelet expansion are available in the literature. The aim of the first approach is to expand the highest order fractional derivative included in the differential equation directly into Haar wavelets, i.e., direct conversion of the Chen and Hsiao approach for fractional differential equations. In [34–38], the Haar wavelet operational matrix of fractional order integration is introduced and implemented for solving differential and integro-differential equations. The aim of the second approach is to utilize the definitions of fractional derivatives (Caputo derivative, etc.) and convert fractional differential terms into integrals, which contain integer derivatives only. Such an approach has been introduced by Lepik in [22] and utilized in a number of papers [39–41]. The two approaches considered are implemented and compared in [42]. It is pointed out in [42] that the two approaches have the same rate of convergence if the order of the fractional derivative exceeds one ( $\alpha > 1$ ). However, if the order of the fractional derivative is less than one ( $\alpha < 1$ ), the second approach has the rate of convergence equal to two, but the rate of convergence of the first approach is  $1 + \alpha$ , i.e., less than two. Thus, in the case of  $\alpha < 1$ , the second approach has a higher convergence rate and can be preferred.

HWM with a nonuniform grid was introduced in [43] using a proportionally changing grid size. The same approach was utilized for the free vibration analysis of non-uniform axially graded beams in [44] and for solving singularly perturbed differential difference equations of neuronal variability in [45].

In most of the studies [17–45], it was concluded that HWM is simple to implement. In the review paper [46], it was pointed out that the HWM is efficient and powerful in solving a wide class of linear and nonlinear reaction–diffusion equations. However, the convergence theorem and accuracy estimates derived for the HWM in [47, 48] state that the order of convergence of the Chen and Hsiao approach-based HWM is equal to two. The latter result is rather modest in the context of engineering. Comparison of the HWM with widely used numerical

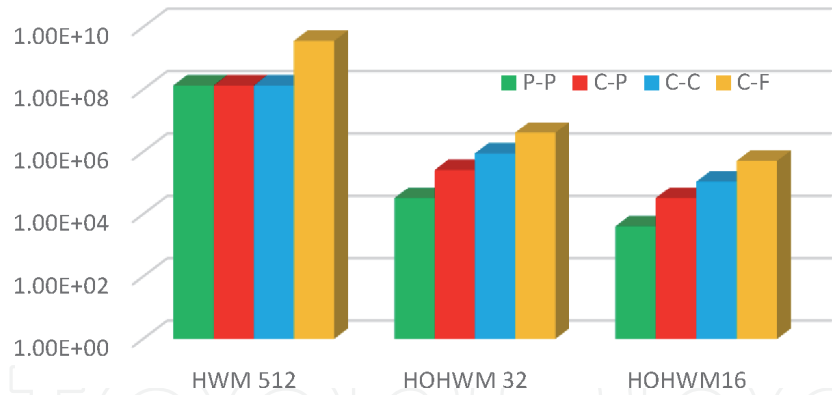


**Figure 1.**  
 Numerical complexity. Free vibration analysis of the nanobeam.

methods in engineering reveals that HWM needs principal improvement in order to compete with the differential quadrature method (DQM) [49].

The HOHWM as an improvement of HWM was recently introduced by Majak et al. in [50]. The convergence rate of the method was improved from 2 to 2 + 2 s, where s stands for the method parameter. This new method is currently underused, but the first results obtained have shown that a principal growth of the accuracy can be achieved with a minimum growth of complexity [51–53]. In [52], the free vibrations analysis of the Euler-Bernoulli nanobeam was performed. **Figure 1** shows the numerical complexity estimates of the HWM and HOHWM solutions yielding a similar absolute error. Here the numerical complexity is determined by number of main operations of the most complex subtask - solution of discrete algebraic system of equations [52].

The logarithmic scale is used in **Figure 1** since the complexity of the HWM appears several orders higher (10<sup>8</sup>) than that of the HOHWM (10<sup>3</sup> ... 10<sup>5</sup>). These results were obtained using the method parameter s = 1 (i.e., fourth order convergence). In practice, one of most important factors is the computational cost. In the case of the considered problem, the computational cost of the HOHWM solution is 10<sup>3</sup> ... 10<sup>5</sup> times lower than that of the HWM. The obtained results hold good in the case of all four boundary conditions considered: pinned-pinned (P–P), clamped-pinned (C–P), clamped-clamped (C–C), and clamped-free (C–F).

## 2. Theoretical basis of the HWM and the HOHWM

This section introduces the Haar functions and presents the theoretical basis of both, the HWM and the HOHWM, covering basic principles, algorithms, convergence and accuracy issues.

### 2.1 Haar functions

The HWM and the HOHWM use different approaches, but both use Haar function expansions for the approximation of derivatives. The Haar functions  $h_i(x)$ , are given as in [14].

$$h_i(x) = \begin{cases} 1 & \text{for } x \in [\xi_1(i), \xi_2(i)) \\ -1 & \text{for } x \in [\xi_2(i), \xi_3(i)) \\ 0 & \text{elsewhere} \end{cases} \tag{1}$$

where  $i = m + k + 1$ ,  $m = 2^j$  is a maximum number of square waves deployed in the interval  $[A, B]$  and the parameter  $k$  indicates the location of the particular square wave,

$$\xi_1(i) = A + 2k\mu\Delta x, \xi_2(i) = A + (2k + 1)\mu\Delta x, \xi_3(i) = A + 2(k + 1)\mu\Delta x, \quad (2)$$

$$\mu = M/m, \Delta x = (B - A)/(2M), M = 2^j. \quad (3)$$

In Eq. (3)  $M = 2^j$  stands for maximum resolution. Obviously, the Haar functions  $h_i(x)$  form an orthonormal basis. The integrals of order  $n$  of the Haar functions (1) can be expressed as in [17]

$$p_{n,i}(x) = \begin{cases} 0 & \text{for } x \in [A, \xi_1(i)) \\ \frac{(x - \xi_1(i))^n}{n!} & \text{for } x \in [\xi_1(i), \xi_2(i)) \\ \frac{(x - \xi_1(i))^n - 2(x - \xi_2(i))^n}{n!} & \text{for } x \in [\xi_2(i), \xi_3(i)) \\ \frac{(x - \xi_1(i))^n - 2(x - \xi_2(i))^n + (x - \xi_3(i))^n}{n!} & \text{for } x \in [\xi_3(i), B) \\ 0 & \text{elsewhere} \end{cases} \quad (4)$$

Formulas (4) hold for a general case where  $i > 1$ , in the case  $i = 1$  holds  $p_{n,1} = \frac{(x-A)^n}{n!}$ . The interval  $[A, B]$  in Eqs. (1)–(3) can be converted to the unit interval  $[0, 1]$  by use of the exchange of variables  $\tau = (x - A)/(B - A)$ .

In the case of uniform mesh the collocation points can be introduced as.

$$x_l = \frac{2l - 1}{4M}, l = 1, \dots, 2M. \quad (5)$$

The elements of the discrete  $2M \times 2M$  Haar matrix can be expressed as values of Haar functions in collocation points given by Eq. (5)

$$H_{il}^{2M} = h_i(x_l). \quad (6)$$

The elements of the matrix of  $n$ -th order integrals of the Haar function can be evaluated as

$$(P_n)_{il}^{2M} = p_{n,i}(x_l), \quad (7)$$

where  $p_{n,i}(x)$  is defined by formulas (4).

## 2.2 Haar wavelet method (HWM)

The Chen and Hsiao approach based HWM, utilized in [15–49]. can be considered as a commonly/widely used HWM.

### 2.2.1 Method description

Let us consider first the  $n$ -th order ordinary differential equation in the general form as.



$$G(x, u, u', u'', \dots, u^{(n-1)}, u^{(n)}) = 0. \quad (8)$$

Let us assume that  $f(x)$  is an integrable square and finite function. The Haar wavelet expansion for the function  $f(x)$  is given as (here  $a_i$  stand for the unknown wavelet coefficients).

$$f(x) = \sum_{i=1}^{\infty} a_i h_i(x). \quad (9)$$

According to the HWM approach introduced by Chen and Hsiao in [15, 16] the highest order derivative involved in Eq. (8) is expanded into the series of Haar wavelets, i.e.,

$$\frac{d^n u(x)}{dx^n} = \sum_{i=1}^{\infty} a_i h_i(x), \quad (10)$$

Based on the definition of the Haar function (1)–(3), Eq. (10) can be expressed as.

$$\frac{d^n u(x)}{dx^n} = a_1 h_1 + \sum_{j=0}^{\infty} \sum_{k=0}^{2^j-1} a_{2^{j+k+1}} h_{2^{j+k+1}}(x). \quad (11)$$

The solution of the differential Eq. (8) can be obtained by integrating Eq. (11)  $n$ -times as.

$$u(x) = \frac{a_1 x^n}{n!} + \sum_{j=0}^{\infty} \sum_{k=0}^{2^j-1} a_{2^{j+k+1}} p_{n,2^{j+k+1}}(x) + B_T(x). \quad (12)$$

In Eq. (12)  $p_{n,2^{j+k+1}}(x)$  stand for  $n$ -th order integrals of the Haar functions given by Eq. (4) and  $B_T(x)$  is a boundary term. Obviously, in the numerical analysis the finite number of the terms corresponding to the fixed maximum resolution ( $N = 2M$ ) can be considered as.

$$u(x) = \frac{a_1 x^n}{n!} + \sum_{j=0}^{2M} \sum_{k=0}^{2^j-1} a_{2^{j+k+1}} p_{n,2^{j+k+1}}(x) + B_T(x). \quad (13)$$

The integration constants included in the boundary term  $B_T(x)$  can be determined from the boundary conditions. Substituting the solution (13) and its derivatives in the differential Eq. (8) and employing discrete collocation points (5), we obtain  $2M \cdot 2M$  algebraic system of equations for determining unknown wavelet coefficients  $a_i$ . Finally, when the wavelet coefficients  $a_i$  are known, the solution of the differential Eq. (8) can be evaluated using expression (13). Note that the collocation points defined by Eq. (5) correspond to uniform mesh. Obviously, various non-uniform meshes can be utilized instead of Eq. (5).

Let us consider next a partial differential equation in the general form as

$$R\left(x, y, \frac{\partial u}{\partial x}, \frac{\partial u}{\partial y}, \frac{\partial^2 u}{\partial x^2}, \frac{\partial^2 u}{\partial y^2}, \frac{\partial^2 u}{\partial x \partial y}, \dots, \frac{\partial^{n+q} u}{\partial x^n \partial y^q}\right) = 0, \quad (14)$$

where  $n$  and  $p$  stand for the highest order derivatives with respect to  $x$  and  $y$ , respectively. The solution domain is considered rectangle  $[0, L_1] \times [0, L_2]$ . According

to the Chen and Hsiao approach the highest order derivative involved in the differential equation is expanded into Haar wavelets (in this case of 2D expansion)

$$\frac{\partial^{n+q}u}{\partial x^n \partial y^q} = \sum_{i=1}^{2M_1} \sum_{l=1}^{2M_2} a_{il} h_i(x) h_l(y). \quad (15)$$

In Eq. (15)  $2M_1$  and  $2M_2$  stand for the number of grid points with respect to  $x$  and  $y$  coordinates, respectively. Such a 2D wavelet expansion was introduced by Lepik in [19] and is most commonly used. Similar to the 1D case, integrating the relation (15)  $n$ -times with respect to  $x$  and  $q$  times with respect to  $y$ , we obtain the solution of the differential Eq. (14) as [19].

$$u(x, y) = \sum_{i=1}^{2M_1} \sum_{l=1}^{2M_2} a_{il} p_{n,i}(x) p_{q,l}(y) + B_T(x, y). \quad (16)$$

The boundary term  $B_T(x, y)$  includes  $n + q$  integration constants which can be determined from the boundary conditions. Substituting Eq. (16) in the differential Eq. (14) and satisfying the obtained equation at the collocation points (e.g., in uniform grid points), we obtain an algebraic system of rank  $(2M_1)^2 \cdot (2M_2)^2$  with respect to the wavelet coefficients. By substituting the wavelet coefficients in Eq. (16), the solution of the differential Eq. (14) can be evaluated at any point in the given domain.

### 2.2.2 Convergence theorem and accuracy estimates

The convergence theorem for the Chen and Hsiao based HWM was proved by Majak et al. in [47].

**Theorem.** Let us assume that  $f(x) = \frac{d^n u(x)}{dx^n} \in L^2(R)$  is a continuous function on  $[0, 1]$  and its first derivative is bounded.

$$\forall x \in [0, 1] \quad \exists \eta : \left| \frac{df(x)}{dx} \right| \leq \eta, n \geq 2 \text{ (boundary value problems)}. \quad (17)$$

Then, the Haar wavelet method based on the approach proposed by Chen and Hsiao in [15, 16] will be convergent, i.e., the  $L^2$ -norm of the error function  $|E_M|$  vanishes as  $J$  goes to infinity. The order of convergence is equal to two.

$$\|E_M\|_2 = O \left[ \left( \frac{1}{2^{J+1}} \right)^2 \right]. \quad (18)$$

The proof is given in [47]. The error bound is derived as.

$$\|E_M\|_2 \leq \frac{\eta C_n}{6} \left( \frac{1}{2^{J+1}} \right)^2 = \frac{4}{9} \frac{\eta}{(\text{floor}(n/2)!)^2} \left( \frac{1}{2^{J+1}} \right)^2. \quad (19)$$

In the particular case where  $n = 1$ , the error bound can be derived as.

$$\|E_M\|_2 \leq \frac{\eta}{\sqrt{3}} \left( \frac{1}{2^{J+1}} \right)^2. \quad (20)$$

The error bounds (19) and (20) are main/biggest error terms determining the rate of convergence. A detailed accuracy analysis of the HWM for the fourth order ordinary differential equations is performed in [48], where two error terms are pointed out as.

$$\|E_M\|_2 \leq \frac{\eta}{12} \left[ \left( \frac{1}{N} \right)^2 + \frac{1}{28} \left( \frac{1}{N} \right)^4 \right]. \quad (21)$$

It appears that the second error term is the fourth order term, which does not play any role in the standard HWM application. However, this information is important in cases where extrapolation is employed for obtained solutions. For example, by applying the Richardson extrapolation, the first error term is canceled and the order of convergence increases from two to four (the value three is omitted since the third order term in error estimate is missing). Furthermore, it has been shown in [48] that the error estimate includes even order terms only. This aspect can be considered in further improvement of the HWM.

Obviously, at the same assumptions, the multi-dimensional Haar wavelet method is also convergent and the rate of convergence is equal to two.

The obtained results will be validated by a number of case studies by computing the numerical rates of convergence and comparing the obtained and theoretical results. These results are confirmed in [47–53] and in other papers.

## 2.3 Higher order Haar wavelet method

As mentioned above, the HOHWM was introduced in [50] as an improvement of the widely used Chen and Hsiao approach based HWM. The HOHWM is based on:

- higher order wavelet expansion,
- algorithm for determining complementary integration constants.

It can be pointed out that utilizing the higher order wavelet expansion itself does not provide substantial increase of the rate of convergence and accuracy. The algorithm used for determining complementary integration constants plays key role.

### 2.3.1 Method description

Let us consider first the  $n$ -th order ordinary differential Eq. (8). According to the the Haar wavelet expansion is expressed as.

$$\frac{d^{n+2s}u(x)}{dx^{n+2s}} = \sum_{i=1}^{\infty} a_i h_i(x), s = 1, 2, \dots \quad (22)$$

In the simplest case, where  $s = 1$ , the  $n + 2$  order derivative is expanded into Haar wavelets. The even values  $2s$  are used, based on the analysis of error estimates of the HWM given in the previous section. Integrating the expression (22)  $n + 2$  times with respect to  $x$  we obtain the solution of the differential Eq. (8) as.

$$u(x) = \frac{a_1 x^{n+2s}}{(n+2s)!} + \sum_{j=0}^{\infty} \sum_{k=0}^{2^j-1} a_{2^j+k+1} p_{n+2s, 2^j+k+1}(x) + S_{BT}(x) + H_{BT}(x). \quad (23)$$



The boundary terms  $S_{BT}(x)$  and  $H_{BT}(x)$  include  $n + 2s$  integration constants  $c_r$ .

$$S_{BT}(x) = \sum_{r=0}^{n-1} c_r \frac{x^r}{r!}, H_{BT}(x) = \sum_{r=n}^{n+2s-1} c_r \frac{x^r}{r!}. \quad (24)$$

The integration constants  $c_0, c_1, \dots, c_{n-1}$  can be determined from the boundary conditions. To determine the remaining  $2s$  integration constants, the following two algorithms are proposed by authors in [50].

Using selected uniform grid points (nearest to the boundary from both sides).

$$x_i = \frac{i}{N}, x_i = 1 - \frac{i}{N}, i = 0, \dots, s-1. \quad (25)$$

Using selected Chebyshev–Gauss–Lobatto grid points (nearest to the boundary from both sides).

$$x_i = \frac{1}{2} \left[ 1 - \cos \frac{(i-1)\pi}{(N-1)} \right], i = 1, \dots, s, i = N-s+1, \dots, N. \quad (26)$$

In the particular case  $s = 1$  the differential Eq. (8) is satisfied in the boundary points.

$$\begin{aligned} &G\left(0, u(0), u'(0), u''(0), \dots, u^{(n-1)}(0), u^{(n)}(0)\right) \\ &= 0, G\left(1, u(1), u'(1), u''(1), \dots, u^{(n-1)}(1), u^{(n)}(1)\right) = 0. \end{aligned} \quad (27)$$

Obviously in the latter case the two algorithms considered above, coincide.

### 3. Numerical convergence analysis and Richardson extrapolation

The derivations of the numerical estimates of the order of convergence, as well as extrapolation formulas can be found in [54] and are omitted herein for the sake of conciseness. Let us denote the numerical solutions on a sequence of nested grids by  $F_{i-2}, F_{i-1}, F_i$ , corresponding to grid sizes  $h_{i-2}/h_{i-1} = h_{i-1}/h_i = 2$ . Then the order of convergence of the numerical method can be estimated by the formula.

$$k_i^E = \log \left( \frac{F_{i-1} - F_{exact}}{F_i - F_{exact}} \right) / \log(2), \quad (28)$$

if the exact solution  $F_{exact}$  is known. If the exact solution is unknown, the following formula can be employed [54].

$$k_i = \log \left( \frac{F_{i-2} - F_{i-1}}{F_{i-1} - F_i} \right) / \log(2). \quad (29)$$

The accuracy of the results can be improved by employing the Richardson extrapolation formula as [54].

$$R_i = F_i + \frac{F_i - F_{i-1}}{2^k - 1}. \quad (30)$$

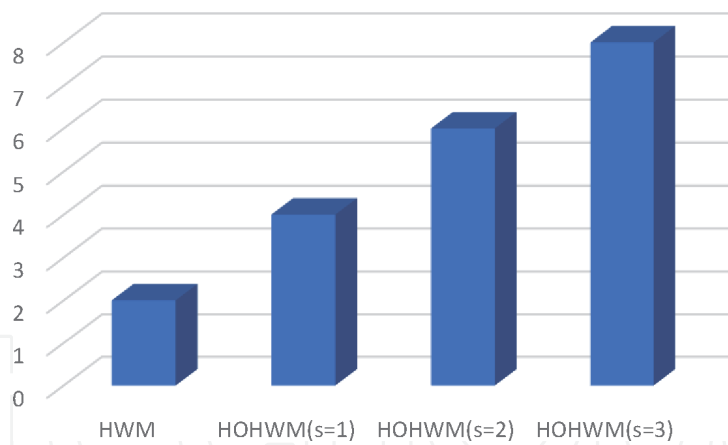


**Figure 2.**  
 Numerical rates of convergence for the HWM and the HOHWM.

The accuracy of the extrapolated results  $R_i$  can be estimated by applying formulas (28) or (29) to these results. The numerical rates of convergence computed for case study, described in Section 5.1, are depicted in **Figure 2**.

The numerical rates of convergence determined are in agreement with convergence theorem for the HWM (Section 2.2.2) and relation given for the HOHWM in Section 2.3 (the rate of convergence of the HOHWM is equal to  $2 + 2s$ ).

#### 4. Complexity analysis

As pointed out above, the accuracy and numerical/time complexity are two key characteristics for any numerical method, algorithm. The computing time is often used as a measure of complexity of algorithms using particular software. More general approach applied commonly in algorithm theory is to estimate the number of basic operations required by each algorithm. The latter approach is independent of software used and does not even require execution of the algorithms. For this reason, in the current study the numerical complexity of the algorithms is estimated based on the number of basic operations.

According to the HWM and the HOHWM algorithms the solution of the differential equation is obtained from the solution of the discrete algebraic system of equations and certain additional operations for composing the linear system and evaluation of the solution in given points. The mentioned additional operations are similar for both methods and have lower asymptotic complexity than the solution of the algebraic system of equations. Thus, the numerical complexity of the HWM and the HOHWM can be compared based on number of basic operations needed for solving algebraic system of equations determined by the rank of the algebraic system of equations (systems are similar by structure).

In the case of the same number of collocations points  $N$ , the ranks of the algebraic systems corresponding to the HWM and the HOHWM are equal to  $N$  and  $N + 2s$  (here  $s = 1, 2$  or  $3$ ), respectively. Furthermore, in the cases where the  $2s$  complementary integrations constants are determined analytically, the rank of the algebraic system of equations of the HOHWM reduces to  $N$ . Thus, in the case of the same mesh used the numerical complexity of the HWM and HOHWM is similar (or equal depending on implementation). However, these solutions have principally different accuracy (see **Tables 1-5**) and such comparison is rather theoretical.

In practice, it is important to compare methods, providing the same accuracy. In the following the given accuracy is fixed by absolute error less than  $2.0e-10$  and the complexities of the HWM and the HOHWM are compared in **Figure 3**. The

HWM				Extrapolated results		
N	Solution at point t = 0.5	Absolute error	Converg. rate	Solution at point t = 0.5	Absolute error	Converg. rate
4	0.60256316864	1.72E-03				
8	0.60386098486	4.27E-04	2.0150	0.60429211947	4.49E-06	
16	0.60418124220	1.06E-04	2.0037	0.60428798114	3.56E-07	3.6598
32	0.60426104700	2.66E-05	2.0009	0.60428765000	2.44E-08	3.8645
64	0.60428098202	6.64E-06	2.0002	0.60428762718	1.59E-09	3.9385
128	0.60428596477	1.66E-06	2.0001	0.60428762569	1.02E-10	3.9680
256	0.60428721039	4.15E-07	2.0000	0.60428762560	6.40E-12	3.9901

**Table 1.**  
*HWM results and extrapolated results (Richardson extrapolation).*

HOHWM(s = 1)				HOHWM (s = 2, VPA)		
N	Solution at point t = 0.5	Absolute error	Converg. rate	Solution at point t = 0.5	Absolute error	Converg. rate
4	0.60426829567	1.93E-05		0.60428745306474	1.73E-07	
8	0.60428616352	1.46E-06	3.7247	0.60428762225323	3.34E-09	5.6915
16	0.60428752673	9.89E-08	3.8865	0.60428762553096	6.06E-11	5.7827
32	0.60428761918	6.41E-09	3.9477	0.60428762559057	1.03E-12	5.8780
64	0.60428762518	4.08E-10	3.9748	0.60428762559158	1.68E-14	5.9367
128	0.60428762557	2.56E-11	3.9876	0.60428762559160	2.69E-16	5.9679
256	0.60428762559	1.60E-12	4.0076	0.60428762559160	4.25E-18	5.9853

**Table 2.**  
*HOHWM (s = 1) and HOHWM (s = 2,VPA).*

HOHWM (s = 3,VPA)			
N	Solution at point t = 0.5	Absolute error	Converg. rate
4	0.604287625766393	1.75E-10	
8	0.604287625565219	2.64E-11	2.7282
16	0.604287625591526	7.19E-14	8.5195
32	0.604287625591597	2.18E-16	8.3631
64	0.604287625591598	7.32E-19	8.2201
128	0.604287625591598	2.69E-21	8.0890
256	0.604287625591598	9.17E-23	4.8738

**Table 3.**  
*HOHWM (s = 3,VPA).*

logarithmic scale is used in **Figure 3**, since the complexities of the HWM and the HOHWM differ by several magnitudes.

In the case of the HWM the absolute error 2.0e-10 was reached by use of 16,384 collocation points (corresponding algebraic system has 16,384 equations). In the case of the HOHWM the same accuracy was achieved by use just 64, 16 or 4

HWM				HOHWM (s = 1)		
N	Solution at point x = 0.5	Absolute error	Converg. rate	Solution at point x = 0.5	Absolute error	Converg. rate
4	5.5271847185	9.63E-02		5.4468387805	1.59E-02	
8	5.4504966936	1.96E-02	2.2961	5.4315095153	6.20E-04	4.6851
16	5.4355789218	4.69E-03	2.0639	5.4309280380	3.85E-05	4.0087
32	5.4320493805	1.16E-03	2.0155	5.4308919203	2.40E-06	4.0053
64	5.4311787173	2.89E-04	2.0038	5.4308896716	1.50E-07	4.0014
128	5.4309617728	7.23E-05	2.0010	5.4308895312	9.36E-09	4.0003
256	5.4309075816	1.81E-05	2.0002	5.4308895225	5.85E-10	4.0001
512	5.4308940366	4.51E-06	2.0001	5.4308895219	3.66E-11	3.9999
1024	5.4308906505	1.13E-06	2.0000	5.4308895219	2.29E-12	3.9968

**Table 4.**  
 Comparison of the HWM and the HOHWM (s = 1).

HWM				HOHWM (s = 1)		
N	Solution at point x = 0.5	Absolute error	Converg. rate	Solution at point x = 0.5	Absolute error	Converg. rate
4	7.9429919221	2.31E-01		7.7081052185	4.12E-03	
8	7.7555236804	4.33E-02	2.4139	7.7125990532	3.78E-04	3.4430
16	7.7224700620	1.02E-02	2.0789	7.7122525729	3.19E-05	3.5669
32	7.7147496939	2.53E-03	2.0189	7.7122227612	2.12E-06	3.9125
64	7.7128508612	6.30E-04	2.0047	7.7122207750	1.34E-07	3.9795
128	7.7123780687	1.57E-04	2.0012	7.7122206490	8.43E-09	3.9949
256	7.7122599897	3.93E-05	2.0003	7.7122206411	5.27E-10	3.9986
512	7.7122304774	9.84E-06	2.0001	7.7122206406	3.30E-11	3.9974
1024	7.7122230998	2.46E-06	2.0000	7.7122206406	2.13E-12	3.9573

**Table 5.**  
 Comparison of the HWM and the HOHWM (s = 1).

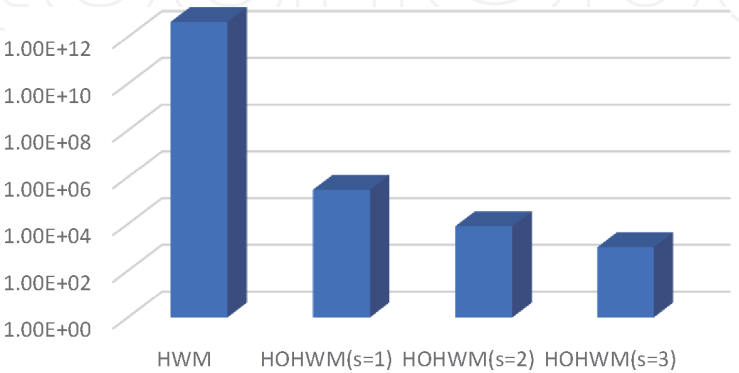


**Figure 3.**  
 Numerical complexities of the HWM and the HOHWM.

collocations points corresponding to the s = 1, s = 2 or s = 3, respectively (i.e. the algebraic system needed to solve is reduced to 64, 16 or 4 equations). Thus, it can be

concluded, that making use of the HOHWM instead of the HWM will lead to principal reduction of numerical complexity of the solution.

The practical value of the developed HOHWM approach is reduction of computational cost of the solution by several magnitudes (directly determined by numerical complexity). It should be noted that making use of the HOHWM instead of the HWM, especially in the cases  $s > 1$  will increase implementation complexity, but not substantially.

## 5. Case studies

In the following, the two case studies are performed in order to validate the accuracy and convergence of the recently introduced HOHWM and compare results with HWM.

### 5.1 Linear ordinary differential equations

As a rule, the new methods are validated on the samples where the exact solution is known. Herein, the linear ordinary differential equations are considered as the first sample problem. Let us consider a sample problem solved in [17] by applying the HWM

$$G\left(t, u(t), \frac{du(t)}{dt}, \frac{d^2u(t)}{dt^2}\right) = \frac{d^2u(t)}{dt^2} + \alpha \frac{du(t)}{dt} + \beta u(t) - \gamma f(t) = 0, \quad (31)$$

where  $f(t)$  is a given function ( $f(t) = \cos(2t)$ ),  $p, q$  and  $r$  are constant parameters ( $\alpha = 0.05, \beta = 0.15, \gamma = 1$ ). The initial conditions  $u(0) = 0, \frac{du}{dt}(0) = 1$  are utilized.

In the case of the HWM, the second order derivative is expanded into Haar wavelets as

$$\frac{d^2u(t)}{dt^2} = aH. \quad (32)$$

In Eq. (32),  $a$  and  $H$  stand for the coefficient vector (row vector) and the discrete Haar matrix given by formulas (6), respectively. The solution of the differential Eq. (31) is obtained by integrating relation (32) twice with respect to  $t$  and satisfying initial conditions

$$u(t) = aP_2 + t, \quad (33)$$

where the elements of the matrix  $P_2$  are defined by (7) and the coefficient vector  $a$  is determined by substituting the solution (33) and its derivatives in Eq. (31) as

$$a = (\gamma f(t) - \alpha - \beta t)[H + \alpha P_1 + \beta P_2]^{-1}. \quad (34)$$

In the case of the HOHWM and  $s = 1$ , the fourth order derivative is expanded into Haar wavelets as

$$\frac{d^4u(t)}{dt^4} = aH. \quad (35)$$

The solution of the differential Eq. (31) is obtained by integrating relation (35) four times with respect to  $t$  and satisfying initial conditions



$$u(t) = aP_4 + c_3 \frac{t^3}{6} + c_2 \frac{t^2}{2} + t, \tag{36}$$

The remaining two integration constants in Eq. (36) can be determined by satisfying Eq. (31) at the boundary points  $t = 0$  and  $t = 1$ . The latter two algebraic equations can be added to the algebraic system obtained by substituting the solution (36) and its derivatives in Eq. (31). In the latter case, the algebraic system includes  $2M + 2$  equations. An alternate approach is to determine the remaining two integration constants analytically from the same conditions and replace to algebraic system.

The numerical results obtained by utilizing the HWM and the HOHWM are compared in **Tables 1-3**.

It can be observed from **Tables 1-3** that in the case of the HWM, the order of convergence tends to two and in the case of the HOHWM, it tends to  $2 + 2s$ , i.e., to four if  $s = 1$ , to six if  $s = 2$  and to eight if  $s = 3$ . Use of HOHWM provides a principal increase of accuracy. The maximum accuracy obtained by the use of the HWM at 256 collocation points ( $N = 256$ ) has been achieved by using the HOHWM at 16 collocation points if  $s = 1$ , and at 4 collocation points if  $s = 2$ . In the case of the HOHWM and  $s = 3$ , the accuracy achieved at 4 collocation points was significantly higher than that of the HWM with 256 collocation points.

In **Figure 4** are shown the error ratios for different mesh ( $N = 4, 16, 64$  and  $256$ ). The absolute error of the HWM is divided by error of the HOHWM, where blue, green and gray colors correspond to the HOHWM parameter  $s$  values 1, 2 and 3, respectively. Thus, in the case of mesh  $N = 4$ , making use of the HOHWM instead of the HWM reduced the absolute error  $8.91E+01$  ( $s = 1$ ) to  $9.83E+06$  ( $s = 3$ ) times. In the case of mesh  $N = 256$ , the use of the HOHWM reduced the absolute error  $2.59E+05$  ( $s = 1$ ) to  $4.53E+15$  ( $s = 3$ ) times. Since the error ratio depends strongly on the mesh used, the logarithmic scale was used in **Figure 4**.

The numerical analysis is performed using MATLAB software. Since the accuracy achieved by the use of the HOHWM in the case of  $s = 2$  and  $s = 3$  exceeds the limits of the double precision computing, the variable precision computing (VPA) was used.

Note that this is needed only in the case of particular problems and large mesh where the accuracy exceeds the limits of double precision computing.

5.2 Nonlinear Lienard equations

The nonlinear differential equation given as

$$\frac{d^2u(x)}{dx^2} + f(u) \frac{du(x)}{dx} + g(u) = 0 \tag{37}$$

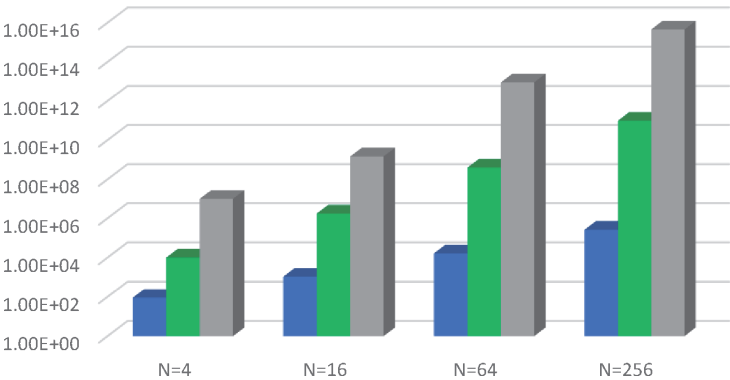


**Figure 4.**  
Ratios of the absolute error of the HWM and the HOHWM.

is known as the Lienard equation. In the following, it is assumed that  $f(u) = 0$  and  $g(u) = 0$ . Let us consider solution in the interval  $[0, 1]$  and assume the boundary conditions in the form.

$$u(0) = u_0, u(1) = u_1. \quad (38)$$

In the current study the nonlinear differential Eq. (37) is linearized by applying the quasi-linearization technique as [55].

$$\frac{d^2 u_{r+1}(x)}{dx^2} + \frac{du_{r+1}(x)}{dx} u_r(x) + \frac{du_r(x)}{dx} u_{r+1}(x) - \frac{du_r(x)}{dx} u_r(x) = 0. \quad (39)$$

Obviously, Eq. (39) can be solved iteratively with respect to  $r$ .

In the case of the HWM, the second order derivative is expanded into Haar wavelets

$$\frac{d^2 u_{r+1}(x)}{dx^2} = aH \quad (40)$$

and the solution of the Lienard Eq. (37) can be derived as

$$u(x) = a_{r+1}P_2 - a_{r+1}xP_2(1) + 2xb_r. \quad (41)$$

In the case of the HOHWM and  $s = 1$  the fourth order derivative is expanded into Haar wavelets

$$\frac{d^4 u_{r+1}(x)}{dx^4} = aH \quad (42)$$

and the solution of the Lienard Eq. (37) can be derived as

$$u(x) = a_{r+1}P_4 - a_{r+1}((b_r y - z)P_4(1) - b_r y P_3(1) - y P_2(1)) + b_r z - b_r^2 y, \\ y = \frac{x^3 - 3x}{6 + 2b_r}, z = \frac{3x}{3 + b_r}. \quad (43)$$

In Eqs. (41) and (43), the value of the parameter  $b_r$  depends on the particular boundary conditions applied. Let us consider first the following boundary conditions.

$$u(0) = 0, u(1) = 6 \tanh(3) \quad (44)$$

then the exact solution is  $u(x) = 6 \tanh(3x)$  and  $b_r = 6 \tanh(3)$ . The results obtained by the use of the HWM and the HOHWM are compared in **Table 4** (point  $x = 0.5$  is used).

Next let us consider the following boundary conditions.

$$u(0) = 0, u(1) = 8 \tanh(4) \quad (45)$$

In the latter case, the exact solution is  $u(x) = 8 \tanh(4x)$  and  $b_r = 8 \tanh(4)$ . The results obtained by the use of the HWM and the HOHWM are compared in **Table 5**.

It can be observed from **Tables 4, 5** that the rates of convergence of the HWM and the HOHWM (with  $s = 1$ ) tend to two and four, respectively. The accuracy obtained using the HWM with maximum resolution  $2M = 1024$  is achieved in the case of the HOHWM with only 32 collocation points.

## 6. Conclusions

The HOHWM introduced recently by authors as an improvement of the HWM in order to compete with the numerical methods widely used in engineering. It was shown that using the HOHWM instead of the HWM will improve principally the accuracy of the solution and increase the rate of convergence in the case of all problems studied. It was found that the rate of convergence of the HOHWM depends on the model parameter  $s$  and is equal to  $2 + 2s$ .

From a practical point of view, it is important that the HOHWM can achieve the same accuracy as the HWM with significantly lower mesh and reduced computational cost.

In the simplest case of the HOHWM where  $s = 1$ , the order of the convergence of the HOHWM is equal to four. The user can select suitable  $s$  value depending on the accuracy requirements of a particular problem considered.

In future study, the new method proposed can be extended/adapted for solving a wide class of differential and integro-differential equations, including fractional differential equations, multidimensional problems, nonlinear boundary value problems arising in engineering design.

## Acknowledgements

The study was supported by Estonian Centre of Excellence in Zero Energy and Resource Efficient Smart Buildings and Districts, ZEBE, TK146 funded by the European Regional Development Fund (grant 2014–2020.4.01.15–0016).

## Author details

Jüri Majak<sup>1\*</sup>, Mart Rataski<sup>1</sup>, Kristo Karjust<sup>1</sup> and Boris Shvartsman<sup>2</sup>

<sup>1</sup> Tallinn University of Technology, Tallinn, Estonia

<sup>2</sup> Estonian Entrepreneurship University of Applied Sciences, Tallinn, Estonia

\*Address all correspondence to: [juri.majak@taltech.ee](mailto:juri.majak@taltech.ee)

## IntechOpen

© 2020 The Author(s). Licensee IntechOpen. This chapter is distributed under the terms of the Creative Commons Attribution License (<http://creativecommons.org/licenses/by/3.0>), which permits unrestricted use, distribution, and reproduction in any medium, provided the original work is properly cited. 

## References

- [1] Mohammadi F, Cattani C, A generalized fractional order Legendre wavelet Tau method for solving fractional differential equations. *Journal of Computational and Applied Mathematics*, 2018;339:306–316.
- [2] Yuttanan B, Razzaghi M, Legendre wavelets approach for numerical solutions of distributed order fractional differential equations. *Applied Mathematical Modelling*, 2019;70:350–364.
- [3] Rayal A, Verma SR, Numerical analysis of pantograph differential equation of the stretched type associated with fractal-fractional derivatives via fractional order Legendre wavelets. *Chaos, Solitons and Fractals*, 2020;139: 110076.
- [4] Jafari H, Yousefi SA, Firoozjaee MA, Momani S, Khalique CM, Application of Legendre wavelets for solving fractional differential equations. *Computers & Mathematics with Applications*, 2011; 62:1038–1045.
- [5] Venkatesh SG, Ayyaswamy SK, Raja Balachandar S, Legendre approximation solution for a class of higher-order Volterra integro-differential equations. *Ain Shams Engineering Journal*, 2012;3:417–422.
- [6] Setia A, Prakash B, Vatsala A, Numerical solution of fourth order fractional integro-differential equation by using Legendre wavelets. *Neural, Parallel and Scientific Computations*, 2015;23(2):377–386.
- [7] Mishra V, and Jindal S, Wavelet Galerkin Solutions of Ordinary Differential Equations. *Int. Journal of Mathematical Analysis*, 2011;5(9): 407–424.
- [8] Shiralashettia SC, Angadib LM, Desh AB, Daubechies Wavelet Based Multigrid and Full Approximation Scheme for the Numerical Solution of Parabolic Partial Differential Equations. *International Journal of Modern Mathematical Sciences*, 2018;16(1):58–75.
- [9] Dehestani H, Ordokhani Y, Razzaghi M, Combination of Lucas wavelets with Legendre–Gauss quadrature for fractional Fredholm–Volterra integro-differential equations. *Journal of Computational and Applied Mathematics*, 2021; 382:113070.
- [10] Sokhal S, Verma SR, A Fourier wavelet series solution of partial differential equation through the separation of variables method. *Applied Mathematics and Computation*, 2020; 388:125480.
- [11] Mohammad M, Trounev A, Implicit Riesz wavelets based-method for solving singular fractional integro-differential equations with applications to hematopoietic stem cell modeling. *Chaos, Solitons & Fractals*, 2020;138: 109991.
- [12] Černá D, Finěk V, Galerkin method with new quadratic spline wavelets for integraal and integro-differential equations. *Journal of Computational and Applied Mathematics*, 2020;363: 426–443.
- [13] Heydari MH, Hooshmandasl MR, Ghaini FMM, A new approach of the Chebyshev wavelets method for partial differential equations with boundary conditions of the telegraph type. *Applied Mathematical Modelling*, 2014; 38(5–6): 1597–1606.
- [14] Haar A, Zur Theorie der orthogonalen Funktionen systeme. *Mathematische Annalen* 1910;69:331–371.
- [15] Chen CF, Hsiao CH, Haar wavelet method for solving lumped and distributed-parameter systems. *IEE Proc Contr Theor Appl* 1997;144(1):87–94.

- [16] Hsiao CH, State analysis of the linear time delayed systems via Haar wavelets. *Math Comput Simulat* 1997;44(5):457–70.
- [17] Lepik Ü. Numerical solution of differential equations using Haar wavelets. *Math Comput Simulat* 2005;68:127–43.
- [18] Lepik Ü, Haar wavelet method for nonlinear integro-differential equations. *Appl Math Comput* 2006;176:324–33.
- [19] Lepik Ü, Solving PDEs with the aid of two dimensional Haar wavelets. *Comput Math Appl* 2011;61:1873–1879.
- [20] Lepik Ü, Application of the Haar wavelet transform to solving integral and differential Equations. *Proc Estonian Acad Sci Phys Math* 2007;56(1):28–46.
- [21] Lepik Ü, Numerical solution of evolution equations by the Haar wavelet method. *Appl Math Comput* 2007;185:695–704.
- [22] Lepik Ü, Solving fractional integral equations by the Haar wavelet method. *Appl Math Comput*, 2009;214(2):468–78.
- [23] Lepik Ü, Hein H, Haar wavelets: with applications. New York: Springer; 2014. 207 p.
- [24] Islam SU, Aziz I, Al-Fhaid AS, An improved method based on Haar wavelets for numerical solution of nonlinear integral and integro-differential equations of first and higher orders. *J Comput Appl Math* 2014;260:449–69.
- [25] Aziz I, Islam SU, Khana F, A new method based on Haar wavelet for the numerical solution of two-dimensional non-linear integral equations. *J Comput Appl Math* 2014;272:70–80.
- [26] Aziz I, Islam SU, New algorithms for the numerical solution of nonlinear Fredholm and Volterra integral equations using Haar wavelets. *J Comput Appl Math* 2013;239(1):333–45.
- [27] Erfanian M, Mansoori A, Solving the nonlinear integro-differential equation in complex plane with rationalized Haar wavelet. *Mathematics and Computers in Simulation*, 2019;165:223–237.
- [28] Majak J, Pohlak M, Eerme M, Application of the Haar Wavelet-based discretization technique to problems of orthotropic plates and shells. *Mech Compos Mater* 2009;45(6):631–42.
- [29] Hein H, Feklistova L, Computationally efficient delamination detection in composite beams using Haar wavelets. *Mech Syst Signal Pr* 2011; 25(6): 2257–70.
- [30] Xie X, Jin G, Ye T, Liu Z. Free vibration analysis of functionally graded conical shells and annular plates using the Haar wavelet method. *Appl Acoust* 2014;85:130–42.
- [31] Xie X, Jin G, Li W, Liu Z, A numerical solution for vibration analysis of composite laminated conical, cylindrical shell and annular plate structures. *Compos Struct* 2014;111:20–30.
- [32] Xie X, Jin G, Yan Y, Shi SX, Liu Z, Free vibration analysis of composite laminated cylindrical shells using the Haar wavelet method, *Compos Struct* 2014;109:169–77.
- [33] Fan J, Huang J, Haar wavelet method for nonlinear vibration of functionally graded CNT-reinforced composite beams resting on nonlinear elastic foundations in thermal environment. *Shock and Vibration*, 2018; 1–16. <https://doi.org/10.1155/2018/9597541>.
- [34] Li Y, Zhao W, Haar wavelet operational matrix of fractional order integration and its applications in



solving the fractional order differential equations, *Applied Mathematics and Computation* 2010;216:2276–2285.

[35] Yi M, Huang J, Wavelet operational matrix method for solving fractional differential equations with variable coefficients. *Applied Mathematics and Computation* 2014;230:383–394.

[36] Chen Y, Yi M, Yu C, Error analysis for numerical solution of fractional differential equation by Haar wavelets method. *Journal of Computational Science* 2012;3:367–373.

[37] Wang L, Ma Y, Meng Z, Haar wavelet method for solving fractional partial differentialequations numerically. *Mathematics and Computation* 2014;227:66–76.

[38] Saeed S Rehman M, Haar wavelet Picard method for fractional nonlinear partialdifferential equations. *Applied MathematicsandComputation*, 2015; 264: 310–322.

[39] Amin R, Shah K, Asif M, Khan I, Ullah F, An efficient algorithm for numerical solution of fractional integro-differential equations via Haar wavelet. *Journal of Computational and Applied Mathematics*, 2021;381:113028.

[40] Abdeljawad T, Amin R, Shah K, Al-Mdallal Q, Jarad F, Efficient sustainable algorithm for numerical solutions of systems of fractional order differential equations by Haar wavelet collocation method. *Alexandria Engineering Journal*, 2020;59(4):2391–2400.

[41] Xie J, Wang T, Ren Z, Zhang J, Quan L, Haar wavelet method for approximating the solution of a coupled system of fractional-order integral–differential equations. *Mathematics and Computers in Simulation*, 2019;163:80–89.

[42] Majak J, Shvartsman B, Pohlak M, Karjust K, Eerme M, Tungel E. Solution of fractional order differential equation

by the Haar Wavelet method.

Numerical convergence analysis for most commonly used approach. *AIP Conference Proceedings*,2016;1738: 480110. DOI: 10.1063/1.4952346.

[43] Lepik Ü, Solving integral and differential equations by the aid of non-uniform Haar wavelets. *Applied Mathematics and Computation*, 20088; 198(1): 326–332.

[44] Hein H, Feklistova L, Free vibrations of non-uniform and axially functionally graded beams using Haar wavelets. *Engineering Structures*, 2011; 33 (12):3696–3701.

[45] Raza A, and Khan A, Non-uniform Haar Wavelet Method for Solving Singularly Perturbed Differential Difference Equations of Neuronal Variability. *Applications and Applied Mathematics*, 2020;6:56–70.

[46] Hariharan G, Kannan K, Review of wavelet methods for the solution of reaction-diffusion problems in science and. *Engineering. Appl Math Model* 2014;38(3):799–813.

[47] Majak J, Shvartsman BS, Kirs M, Pohlak M, Herranen H, Convergence theorem for the Haar wavelet based discretization method. *Composite Structures*, 2015;126:227–232.

[48] Majak J, Shvartsman BS, Karjust K, Mikola M, Haavajõe A, Pohlak M, On the accuracy of the Haar wavelet discretization method. *Composites Part B: Engineering*, 2015;80:321–327.

[49] Kirs M, Karjust K, Aziz I, Ounapuu E, Tungel E, Free vibration analysis of a functionally graded material beam: evaluation of the Haar wavelet method. *Proceedings of the Estonian Academy of Sciences*, 2018;67 (1):1–9.

[50] Majak J, Pohlak M, Karjust K, Eerme M, Kurnitski J, Shvartsman BS,

New higher order Haar wavelet method:  
Application to FGM structures.  
Composite Structures, 2018; 201:72–78.

[51] Majak J, Pohlak M, Eerme M, Shvartsman B, Solving ordinary differential equations with higher order Haar wavelet method. AIP Conference Proceedings, 2019;2116:330002.

[52] Majak J, Shvartsman B, Ratras M, Bassir D, Pohlak M, Karjust K, Eerme M, Higher- order Haar wavelet method for vibration analysis of nanobeams, Materials Today Communications, 2020;25:101290.

[53] Ratras M, Salupere A, Application of Higher Order Haar Wavelet Method for Solving Nonlinear Evolution Equations. Mathematical Modelling and Analysis, 2020;25 (2):271–288. DOI: 10.3846/mma.2020.11112.

[54] Shvartsman B, Majak J, Numerical method for stability analysis of functionally graded beams on elastic foundation. Applied Mathematical Modelling, 2016;40 (4–5):3713–3719.

[55] Ratras M, Application of Haar Wavelet Method for Solving Nonlinear Evolution Equations. AIP Conference Proceedings, 2019;2116:330004. DOI: 10.1063/1.5114342.